Supporting Information

A comparison of the positional effect of difluorination and the synergistic effect of siloxane-terminated side chains on benzodithiophene-based conjugated polymers for efficient photovoltaic application

Qian Wang, Zelong Hu, Lianjie Zhang*, Rihang Qiu, Deng Zhou, Jiahao Liang, Junwu Chen*

Institute of Polymer Optoelectronic Materials & Devices, State Key Laboratory of Luminescent Materials & Devices, South China University of Technology, Guangzhou 510640, P. R. China

EXPERIMENTAL SECTION

General Information

Device Fabrication and Characterization

The device structure was ITO/ZnO/polymer:IT-4F (1:1 by weight)/MoO_3/Al. Patterned indium tin oxide (ITO)-coated glass with a sheet resistance of 15–20 ohm/square was cleaned by a surfactant scrub and then underwent a wet-cleaning process inside an ultrasonic bath that began with deionized water, followed by acetone and 2-propanol. A solution-processed zinic oxide (ZnO) interlayer of 30 nm was spin-coated onto the ITO glass. The optimal active layer solutions (D/A ratio of 1:1) with donor concentration of 8 mg/mL were prepared in CB with 0.5% (volume fraction) of 1,8-diiodooctane. Warm solutions (90 °C) were then spin-coated onto the substrates and dried at 80 °C for 5 min. The thickness values of active layers based on all the polymers were around 100 nm, which were nearly the same as those for the SCLC measurement. A 10 nm MoO_3 layer and a 100 nm Al layer were subsequently evaporated through a shadow mask to define the active area of the devices (5.7 mm^2) and form the top anode. The PCE was determined from *J-V* curve measurements (using a Keithley 2400 sourcemeter) under a 1 sun, AM 1.5G spectrum from a solar simulator (Oriel model 91192; 1000 W m^{-2}). Masks made using laser beam cutting technology to have a well-defined area of 5.7 mm^2 were attached to define the effective area for accurate measurement. All the masked and unmasked tests gave consistent results with relative errors within 5%. The solar simulator illumination intensity was determined using a monocrystal silicon reference cell (Hamamatsu S1133, with KG-5 visible color filter) calibrated by the National Renewable Energy Laboratory (NREL). Theoretical J_{sc} values obtained by integrating the product of the EQE with the AM 1.5G solar spectrum agreed with the measured value to within 5%.

Methods

^{1}H NMR and ^{13}C NMR spectra were recorded on a Bruker AV 500 or 400 spectrometer with tetramethylsilane (TMS) as the internal reference. Mass spectrometer was performed on The Waters acquity TQD ultra performance liquid chromatography triple quadrupole tandem mass spectrometer. The number-average molecular weights (M_n) and the polydispersity index (PDI) of polymers were measured by high temperature gel permeation chromatography (GPC) at 150 °C using 1,2,4-trichlorobenezene as eluent. UV−vis absorption spectra were recorded on an UV-3600 (Shimadzu Co.) spectrophotometer. Cyclic voltammetry was carried out on a CHI660A electrochemical work station with platinum electrodes at a scan rate of 50 mV/s against an Ag/Ag^+ reference electrode with a nitrogen-saturated solution of 0.1 M tetrabutylammonium hexafluorophosphate (Bu_4NPF_6) in acetonitrile. Potentials were referenced to the ferrocenium/ferrocene couple by using ferrocene as an internal standard. Thermogravimetric analysis (TG) was performed on NETZSCH TG 209 in nitrogen, with a heating rate of 20 ºC min^{-1}. The photoluminescence (PL) measurement was performed on a Steady State and Lifetime Modular Spectrofluorometer (HORIBA/Fluorolog-3). The pristine and blend films were spin-coated onto the SiO_2 substrates using identical blend solutions as those used in devices.

Space-Charge Limited Current (SCLC) Measurement

Hole-only and electron-only devices were fabricated to measure the hole and electron mobilities of active layers using the space charge limited current (SCLC) method with hole-only device of ITO/PEDOT:PSS/Active layer/MoO_3/Al and electron-only device of ITO/ZnO/Active layer/PFN-Br/Al. The mobilities (μ) were determined by fitting the dark current to the model of a single carrier SCLC, described by the equation:

$$J = \frac{9}{8}\varepsilon_0\varepsilon_r\mu\frac{V^2}{d^3} \tag{1}$$

where J is the current, ε_0 is the permittivity of free space, ε_r is the material relative permittivity, d is the thickness of the active layer, and V is the effective voltage. The effective voltage can be obtained by subtracting the built-in voltage (V_{bi}) and the voltage drop (V_s) from the substrate's series resistance from the applied voltage (V_{appl}), $V = V_{appl} - V_{bi} - V_s$. The mobility can be calculated from the slope of the $J^{1/2} \sim V$ curves.

Grazing Incidence Wide-Angle X-ray Scattering (GIWAXS) Characterization.

GIWAXS measurements were performed at beamline 7.3.3 at the Advanced Light Source. Samples were prepared on Si substrates using identical blend solutions as those used in devices. The 10 keV X-ray beam was incident at a grazing angle of 0.12°, 0.16°, selected to maximize the scattering intensity from the samples. The scattered x-rays were detected using a Dectris Pilatus 2M photon counting detector.

Contact angle measurements.

The contact angle tests were performed on a Dataphysics OCA40 Micro surface contact angle analyzer. The surface energy of the polymers was characterized and calculated by the contact angles of the two probe liquids using the Wu model (2):

Wu model:

$$\gamma_{water}(1+\cos\theta_{water}) = \frac{4\gamma_{water}^{d}\gamma^{d}}{\gamma_{water}^{d}+\gamma^{d}} + \frac{4\gamma_{water}^{p}\gamma^{p}}{\gamma_{water}^{p}+\gamma^{p}} \tag{2}$$

$$\gamma_{oil}(1+\cos\theta_{oil}) = \frac{4\gamma_{oil}^{d}\gamma^{d}}{\gamma_{oil}^{d}+\gamma^{d}} + \frac{4\gamma_{oil}^{p}\gamma^{p}}{\gamma_{oil}^{p}+\gamma^{p}}$$

$$\gamma = \gamma^{d} + \gamma^{p} \tag{3}$$

where γ is the total surface tension of acceptor and polymers; γ^{d} and γ^{p} are the dispersion and polar components of γ; γ_{i} is the total surface tension of the i material (i = water or diiodomethane); γ_{i}^{d} and γ_{i}^{p} are the dispersion and polar components of γ_{i}; and θ_{i} is the droplet contact angle of the i material on the acceptor and polymers films.

Atomic Force Microscopy and Transmission Electron Microscopy

Tapping-mode atomic force microscopy (AFM) images were obtained using a Nano Scope NS3A system (Digital Instrument) to observe the surface morphology of active layers. Transmission electron microscopy (TEM) images were obtained using JEM-2100F with an accelerating voltage of 30 kV.

Materials

Unless otherwise mentioned, all chemical reagents and materials were purchased from commercial sources and used without further purification.

General Procedures for 4(EH, ET), 5(EH, ET) and 6(EH, ET):

In the anhydrous tetrahydrofuran (THF) solution of compound **1-3(EH, ET)** (3 eq.) under nitrogen atmosphere, the n-Butyllithium (3.3 eq., 2.4M in hexane) was added dropwise at −78 °C. The solution was kept at −78 °C for 2 h, then the benzo[1,2-*b*:4,5-*b'*]dithiophene-4,8-dione (1 eq.) was added as the second reactant. The solution was then wormed to room temperature and stirred for other 8 h. After that, the solution of stannous chloride in dilute hydrochloric acid solution was added slowly, and the solution was stirred overnight. The mixed solution was then washed with deionized water and dichloromethane (DCM). The organic layer was collected and concentrated by rotary evaporator. The mentioned product was purified by column chromatography on silica gel as white solid.

4EH: 1.60 g, 50% yield, when 1.14 g (5 mmol) benzo[1,2-*b*:4,5-*b'*]dithiophene-4,8-dione was used. ^{1}H NMR (400 MHz, $CDCl_3$): δ (ppm): 7.46 (d, J = 5.7 Hz, 2H), 7.35 (d, J = 5.7 Hz, 2H), 7.20 (m, 4H), 2.71 (d, J = 7.2 Hz, 4H), 1.77-1.69 (m, 2H), 1.47-1.25 (m, 16H), 0.94 (m, 12H).

4ET: 3.00 g, 60% yield, when 2.00 g (9 mmol) benzo[1,2-*b*:4,5-*b'*]dithiophene-4,8-dione was used. ^{1}H NMR (400 MHz, $CDCl_3$): δ (ppm): 7.46 (d, J = 5.7 Hz, 2H), 7.34 (d, J = 5.7 Hz, 2H), 7.21 (d, 4H), 5.95-5.85 (m, 2H), 5.13-5.02 (m, 4H), 2.80 (t, J = 7.7 Hz, 4H), 2.21 (q, J = 7.0 Hz, 4H), 1.85-1.76 (m, 4H). ^{13}C NMR (126 MHz, $CDCl_3$): δ (ppm): 162.80, 162.72, 160.83, 160.75, 138.19, 138.00, 135.95, 128.74, 128.01, 122.56, 115.02, 112.29, 112.07, 33.54, 28.68, 22.04.

5EH: 4.29 g, 56% yield, when 2.60 g (12 mmol) benzo[1,2-*b*:4,5-*b'*]dithiophene-4,8-dione was used. ^{1}H NMR (400 MHz, $CDCl_3$): δ (ppm): 7.44 (d, J = 5.6 Hz, 2H), 7.35-7.27 (m, 2H), 7.19-7.16 (m, 2H), 7.14-7.07 (m, 2H), 2.72 (d, J = 7.2 Hz, 4H), 1.77-1.68 (m, 2H), 1.37 (m, 16H), 0.94 (m, 12H).

5ET: 4.20 g, 56% yield, when 3.00 g (13 mmol) benzo[1,2-*b*:4,5-*b'*]dithiophene-4,8-dione was used. ^{1}H NMR (400 MHz, $CDCl_3$): δ (ppm): 7.44 (d, J = 5.6, 2H), 7.36-7.29 (m, 2H), 7.16 (m, 4H), 5.89 (m, 2H), 5.14-5.02 (m, 4H), 2.81 (t, J = 7.7 Hz, 4H), 2.21 (q, J = 7.0 Hz, 4H), 1.90-1.81 (m, 4H). ^{13}C NMR (126 MHz, $CDCl_3$): δ (ppm): 138.54, 138.15, 136.64, 132.18, 132.08, 127.73, 125.71, 125.60, 125.46, 125.26, 123.99, 122.77, 115.21, 77.31, 77.05, 76.80, 33.40, 29.11, 28.46.

6EH: 870 mg, 10% yield, when 3.00 g (13 mmol) benzo[1,2-*b*:4,5-*b'*]dithiophene-4,8-dione was used. ^{1}H NMR (400 MHz, CDCl$_3$): δ (ppm): 7.44 (d, J = 5.6 Hz, 2H), 7.11 (d, J = 5.6 Hz, 2H), 6.93 (d, J = 8.3 Hz, 4H), 2.65 (d, J = 7.1 Hz, 4H), 1.73-1.64 (m, 2H), 1.43-1.25 (m, 16H), 0.93 (m, 12H).

6ET: 937 mg, 15% yield, when 2.50 g (11 mmol) benzo[1,2-*b*:4,5-*b'*]dithiophene-4,8-dione was used. ^{1}H NMR (400 MHz, CDCl$_3$): δ (ppm): 7.44 (d, J = 5.6 Hz, 2H), 7.10 (d, J = 5.6 Hz, 2H), 6.97 (d, J = 7.7 Hz, 4H), 5.93-5.83 (m, 2H), 5.13-5.02 (m,4H), 2.75 (t, J = 7.7 Hz, 4H), 2.19 (q, J = 7.0 Hz, 4H), 1.89-1.80 (m, 4H). ^{13}C NMR (126 MHz, CDCl$_3$): δ (ppm): 161.30, 161.23, 159.31, 159.24, 138.96, 138.07, 137.13, 127.54, 122.54, 119.03, 115.32, 111.97, 111.77, 35.09, 33.20, 29.86.

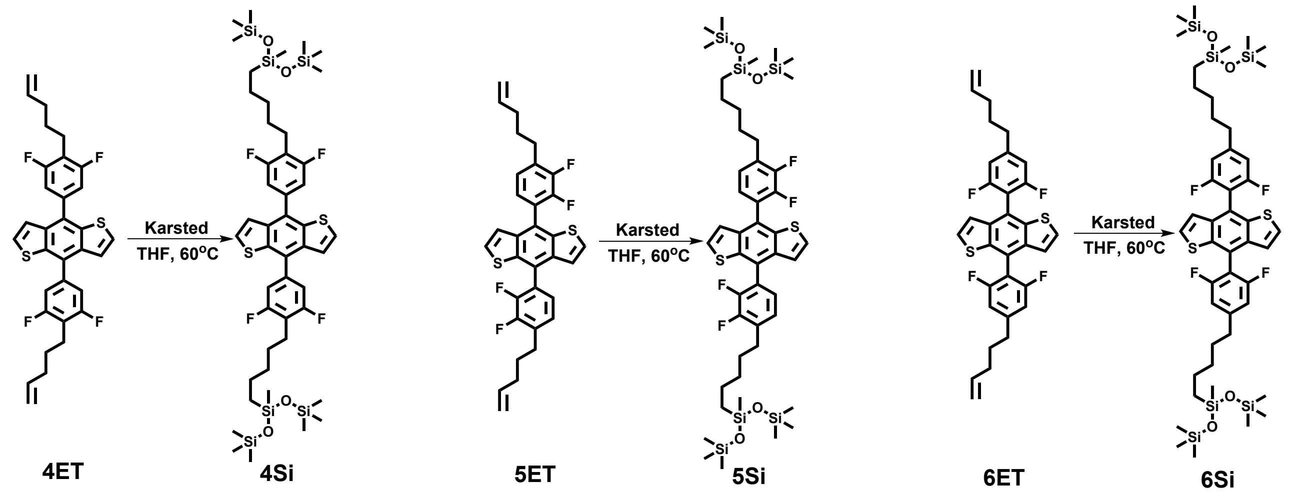

Scheme S1. Synthetic process of 4Si, 5Si and 6Si.

General Procedures for 4Si, 5Si and 6Si.

To the solution of compound **4-6ET** (0.80g，1.5mmol) and 1,1,1,3,5,5,5-Heptamethyltrisiloxane (1.3g, 6mmol) in 8 ml *o*-xylene under nitrogen atmosphere, the Platinum (0)-1,3-diviny-1,1,3,3-tetramethyldisioxane was added as catalyst (5-10 d). The solution was then wormed to 60 °C and stirred overnight. After cooled to the room temperature, the crude product was concentrated and purified by column chromatography on silica gel to get the product as light yellow oil.

4Si: 1.43 g, 96% yield, when 830 mg (1.5 mmol) 4ET was used. ^{1}H NMR (400 MHz, CDCl$_3$): δ (ppm): 7.46 (d, J = 5.7 Hz, 2H), 7.35 (d, J = 5.7 Hz, 2H), 7.21 (d, 4H), 2.78 (t, J = 7.6 Hz, 4H), 1.74 (m, 4H), 1.29-1.25 (m, 8H), 0.54-0.49 (m, 4H), 0.1 (s, 36H), 0.02 (s, 6H).

5Si: 1.37 g, 92% yield, when 830 mg (1.5 mmol) 5ET was used. ^{1}H NMR (400 MHz, CDCl$_3$): δ (ppm): 7.44 (d, J = 5.6 Hz, 2H), 7.36-7.28 (m, 2H), 7.19-7.10 (m, 4H), 2.79 (t, J = 7.6 Hz, 4H), 1.74(m, 4H), 1.49-1.42 (m, 8H), 0.56-0.48 (m, 4H), 0.1 (s, 36H), 0.01 (s, 6H).

6Si: 1.42 g, 95% yield, when 830 mg (1.5 mmol) 6ET was used. ^{1}H NMR (400 MHz, CDCl$_3$): δ (ppm): 7.44 (d, J = 5.6 Hz, 2H), 7.11 (d, J = 5.6 Hz, 2H), 6.96 (d, J = 8.3 Hz, 4H), 2.72 (t, J = 7.6 Hz, 4H), 1.72 (m, 4H), 1.46-1.40 (m, 8H), 0.54-0.49 (m, 4H), 0.1 (s, 36H), 0.02 (s, 6H).

General Procedures for M1-3

In a 100mL 2-neck flask, compound **4-6(EH, Si)** (1 eq.) was dissolved in 25 mL anhydrous THF under nitrogen atmosphere. The solution was cooled to －78 °C and then n-BuLi (3.5 eq., 2.4M in hexane) was added dropwise. The solution was stirred at －78 °C for 2 h. Then the trimethyltin chloride solution (3.5 eq., 1 M in THF) was added, and the mixture was stirred at room temperature overnight. After that, the reaction was stoped by adding the deionized water and the mixture was extracted by DCM for three times. The organic layer was dried over anhydrous MgSO$_4$, and concentrated by rotary evaporator. The crude product was purified by recrystallization from ethyl alcohol. The pure compound **M1-3** was obtained as white solid.

M1EH: 1.16 g, 40% yield, when 1.91 g (3 mmol) 4EH was used. ^{1}H NMR (400 MHz, CDCl$_3$, δ): δ (ppm): 7.32 (s, 2H), 7.21 (d, J = 7.8 Hz, 4H), 2.72 (d, J = 7.2 Hz, 4H), 1.78-1.71 (m, 2H), 1.47-1.30 (m, 16H), 0.97 (t, J = 7.4 Hz, 6H), 0.91 (t, J = 6.9 Hz, 6H), 0.47-0.31 (m, 18H). ^{13}C NMR (126 MHz, CDCl$_3$): δ (ppm): 162.96, 162.87, 160.99, 160.91, 143.12, 142.24, 136.72, 130.02, 127.11, 112.23, 112.01, 39.59, 32.60, 28.76, 27.06, 26.02, 23.00, 14.11, 10.76, -8.31. MS (LC-MS) m/z: calcd. for ($C_{44}H_{58}F_4S_2Sn_2$): 966.20; found: 966.30.

M1Si: 1.59 g, 30% yield, when 3.98 g (4 mmol) 4Si was used. ^{1}H NMR (400 MHz, $CDCl_3$, δ): *δ* (ppm): 7.34 (s, 2H), 7.21 (d, *J* = 7.8 Hz, 4H), 2.78 (t, *J* = 7.7 Hz, 4H), 1.75-1.67 (m, 4H), 1.51-1.41 (m, 8H), 0.54-0.50 (m, 4H), 0.47-0.32 (m, 18H), 0.1 (s, 36H), 0.02 (s, 6H). ^{13}C NMR (126 MHz, $CDCl_3$): *δ* (ppm): 162.76, 162.68, 160.79, 160.71, 143.16, 142.32, 136.77, 130.07, 127.15, 112.32, 112.11, 33.15, 29.41, 22.94, 22.54, 17.60, 1.93, -0.18, -8.25. MS (LC-MS) m/z: calcd. for ($C_{52}H_{86}F_4O_4S_2Si_6Sn_2$): 1321.30; found: 1321.30.

M2EH: 1.12 g, 35% yield, when 1.93 g (3 mmol) 5EH was used. ^{1}H NMR (400 MHz, $CDCl_3$, δ): *δ* (ppm): 7.33-7.27 (m, 2H), 7.15-7.10 (m, 4H), 2.72 (d, *J* = 10.1 Hz, 4H), 1.76-1.71 (m, 2H), 1.47-1.31 (m, 16H), 0.96 (t, *J* = 7.8 Hz, 6H), 0.92 (t, *J* = 6.9, 6H), 0.43-0.29 (m, 18H). ^{13}C NMR (126 MHz, $CDCl_3$): *δ* (ppm): 142.77, 142.70, 137.41, 131.44, 131.34, 130.30, 126.14, 126.03, 125.39, 125.28, 122.23, 40.11, 33.33, 32.55, 28.84, 25.92, 23.00, 14.15, 10.83, -8.29. MS (LC-MS) m/z: calcd. for ($C_{44}H_{58}F_4S_2Sn_2$): 966.20; found: 966.60.

M2Si: 1.27 g, 30% yield, when 2.98 g (3 mmol) 5Si was used. ^{1}H NMR (400 MHz, $CDCl_3$, δ): *δ* (ppm): 7.35-7.28 (m, 2H), 7.16-7.12 (m, 4H), 2.79 (t, *J* = 7.7 Hz, 4H), 1.79-1.72 (m, 4H), 1.50-1.41 (m, 8H), 0.56-0.49 (m, 4H), 0.33 (t, *J* = 28.5 Hz, 18H), 0.09 (s, 36H), 0.02 (s, 6H). ^{13}C NMR (126 MHz, $CDCl_3$): *δ* (ppm): 142.81, 142.69, 137.42, 132.25, 132.15, 130.34, 126.19, 126.08, 125.59, 125.03, 122.28, 33.09, 29.77, 29.00, 22.99, 17.61, 1.94, -0.17, -8.25. MS (LC-MS) m/z: calcd. for ($C_{52}H_{86}F_4O_4S_2Si_6Sn_2$): 1321.30; found: 1322.20.

M3EH: 1.24 g, 50% yield, when 1.60 g (2.5 mmol) 6EH was used. ^{1}H NMR (400 MHz, $CDCl_3$, δ): *δ* (ppm): 7.08 (s, 2H), 6.94 (d, *J* = 8.7 Hz, 4H), 2.65 (d, *J* = 13.1, 4H), 1.74 -1.65 (m, 2H), 1.45-1.30 (m, 16H), 0.96 (t, *J* = 6.9 Hz, 6H), 0.91 (t, *J* = 6.9 Hz, 6H), 0.43-0.27 (m, 18H). ^{13}C NMR (126 MHz, CDCl$_3$): *δ* (ppm): 161.21, 161.16, 159.23, 159.17, 143.11, 142.37, 137.90, 130.11, 117.14, 112.47, 112.33, 40.80, 40.20, 32.43, 28.87, 25.76, 22.96, 14.12, 10.85, -8.31. MS (LC-MS) m/z: calcd. for ($C_{44}H_{58}F_4S_2Sn_2$): 966.20; found: 965.70.

M3Si: 952 mg, 30% yield, when 2.38 g (2.4 mmol) 6Si was used. ^{1}H NMR (400 MHz, CDCl$_3$, δ): *δ* (ppm): 7.10 (s, 2H), 6.96 (d, *J* = 8.2 Hz, 4H), 2.73 (t, *J* = 7.7 Hz, 4H), 1.78-1.71 (m, 4H), 1.50-1.40 (m, 8H), 0.56-0.49 (m, 4H), 0.43-0.28 (m, 18H), 0.1 (s, 36H), 0.03 (s, 6H). ^{13}C NMR (126 MHz, CDCl$_3$): *δ* (ppm): 161.35, 161.29, 159.37, 159.30, 143.17, 142.38, 137.94, 130.18, 117.18, 111.81, 111.62, 35.81, 32.95, 30.50, 23.02, 17.62, 1.95, -0.17, -8.24. MS (LC-MS) m/z: calcd. for ($C_{52}H_{86}F_4O_4S_2Si_6Sn_2$): 1321.30; found: 1320.10.

General procedure of polymerization

Dibromo monomer 1,3-bis(5-bromothiophen-2-yl)-5,7-bis(2-ethylhexyl)benzo[1,2-c:4,5-c']dithiophene-4,8-dione (**M4**, 94.44 mg, 0.2 mmol) and one Bis(trimethyltin) monomer **M1-3(EH, Si)** were mixed in 4 mL o-xylene and 1 mL DMF. After being purged with nitrogen for 30 min, the catalyst Pd (PPh_3)$_4$ (11.55 mg) was added, and the mixture was then purged with nitrogen for another 1 h. The reaction mixture was heated to 110 °C for 24 h. Then the mixture was cooled to room temperature, and the polymer was precipitated by addition of 50 mL methanol and filtered. The precipitate was then subjected to Soxhlet extraction with methanol, dichloromethane, and chloroform. Finally, the polymer was recovered as solid from the chloroform fraction by precipitation with methanol and dried under vacuum. The number-average molecular weights (M_n) and the polydispersity index (PDI) of polymers were measured by high temperature gel permeation chromatography (GPC) at 150 °C using 1,2,4-trichlorobenezene as eluent.

SUPPORTING TABLES AND FIGURES

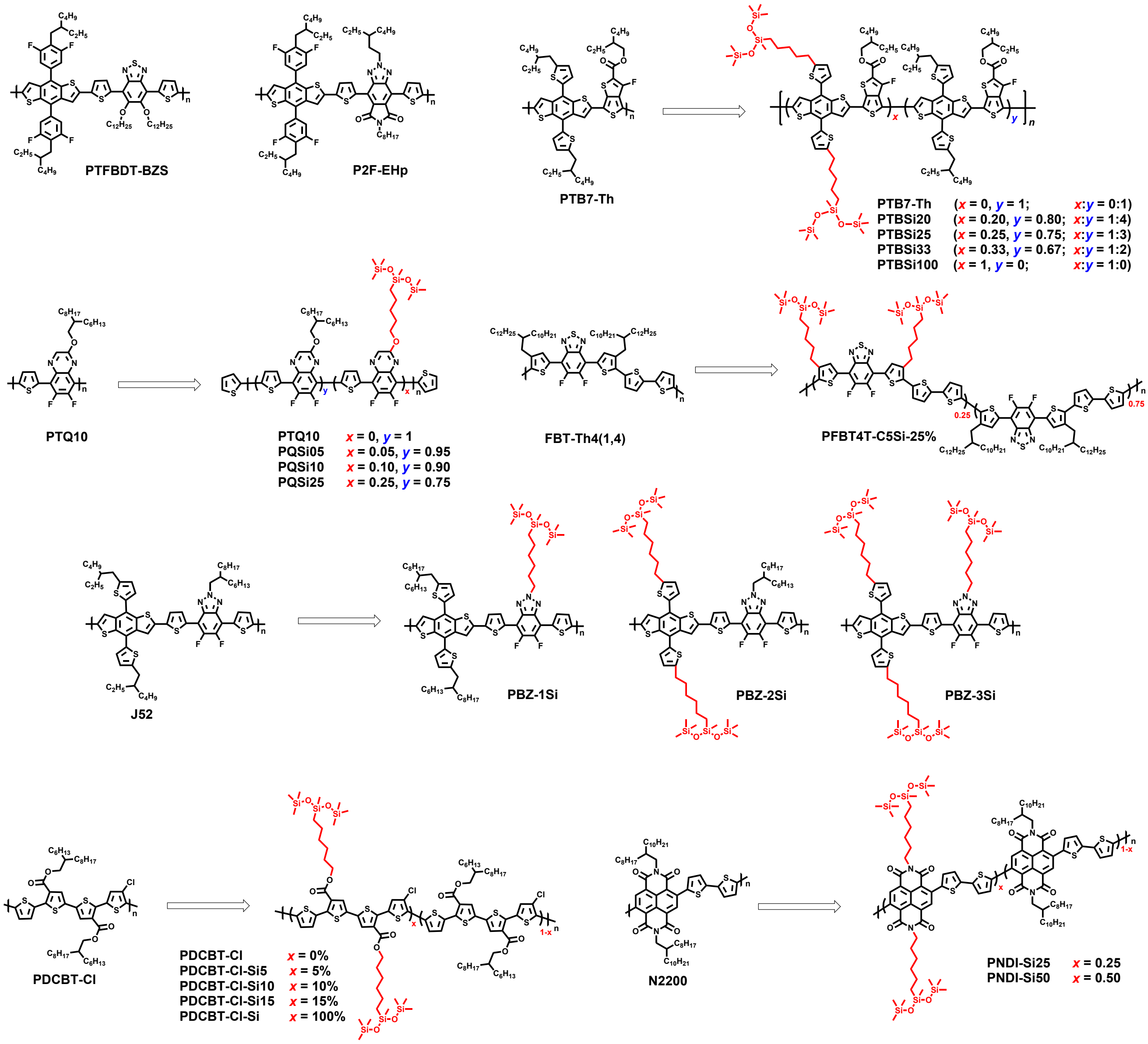

Figure S1. Chemical structures of the mentioned polymers.

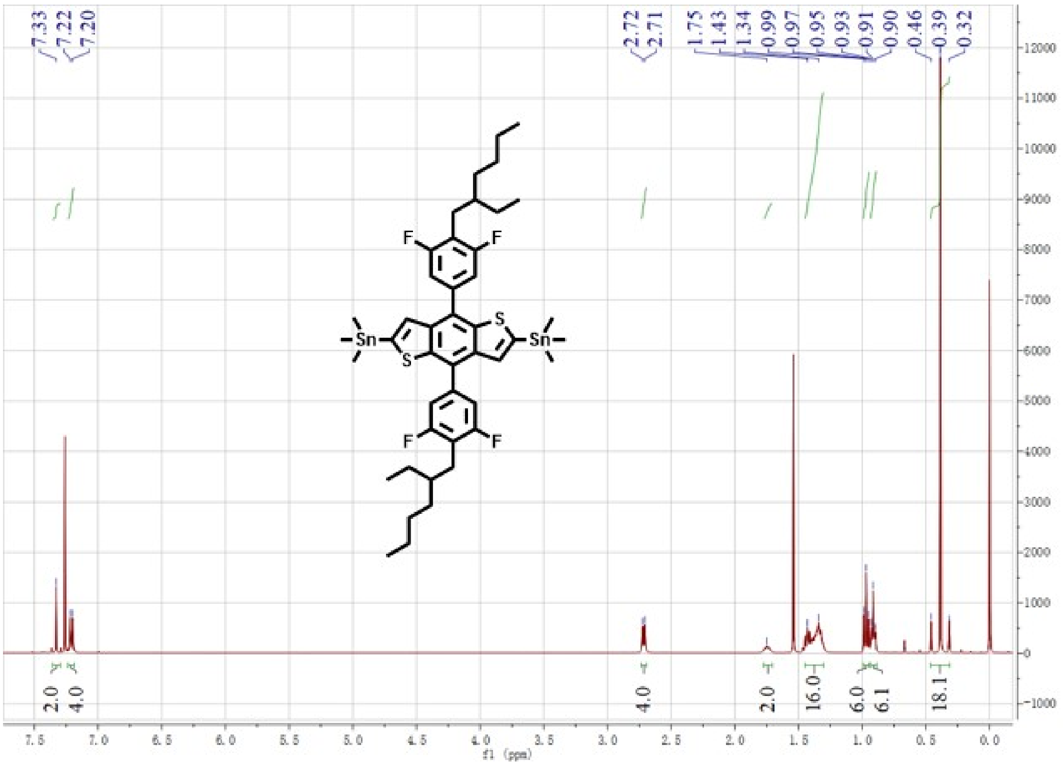

Figure S2. ^{1}H NMR spectrum of compound M1EH in $CDCl_3$.

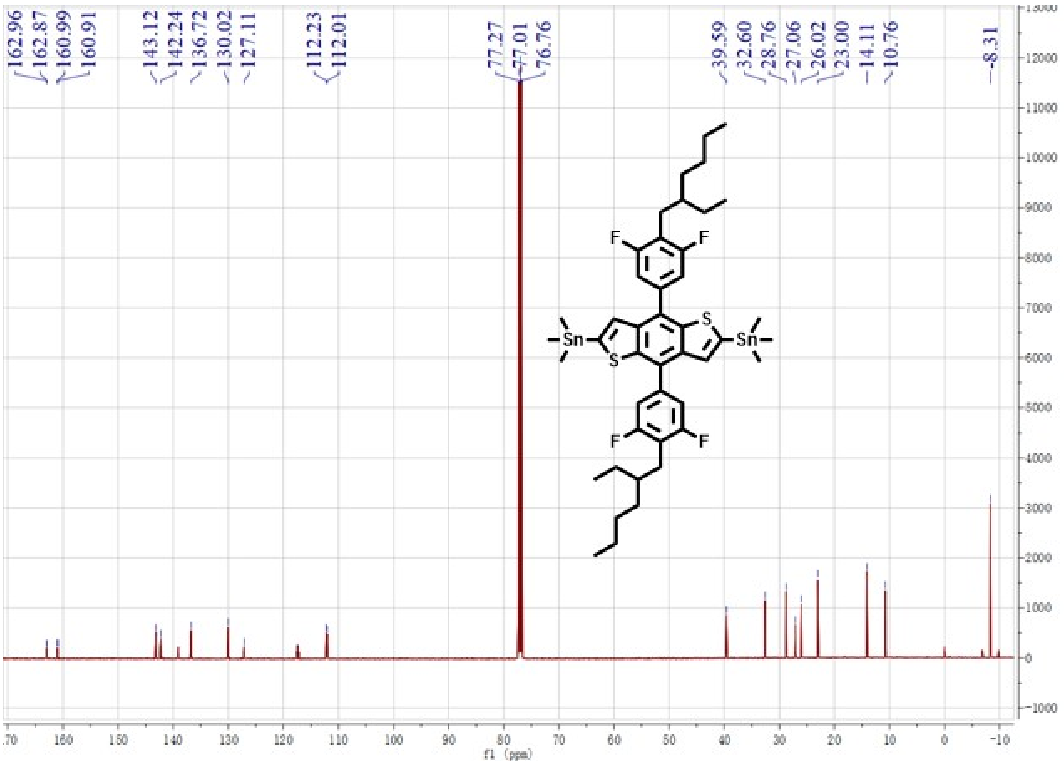

Figure S3. ^{13}C NMR spectrum of compound M1EH in $CDCl_3$.

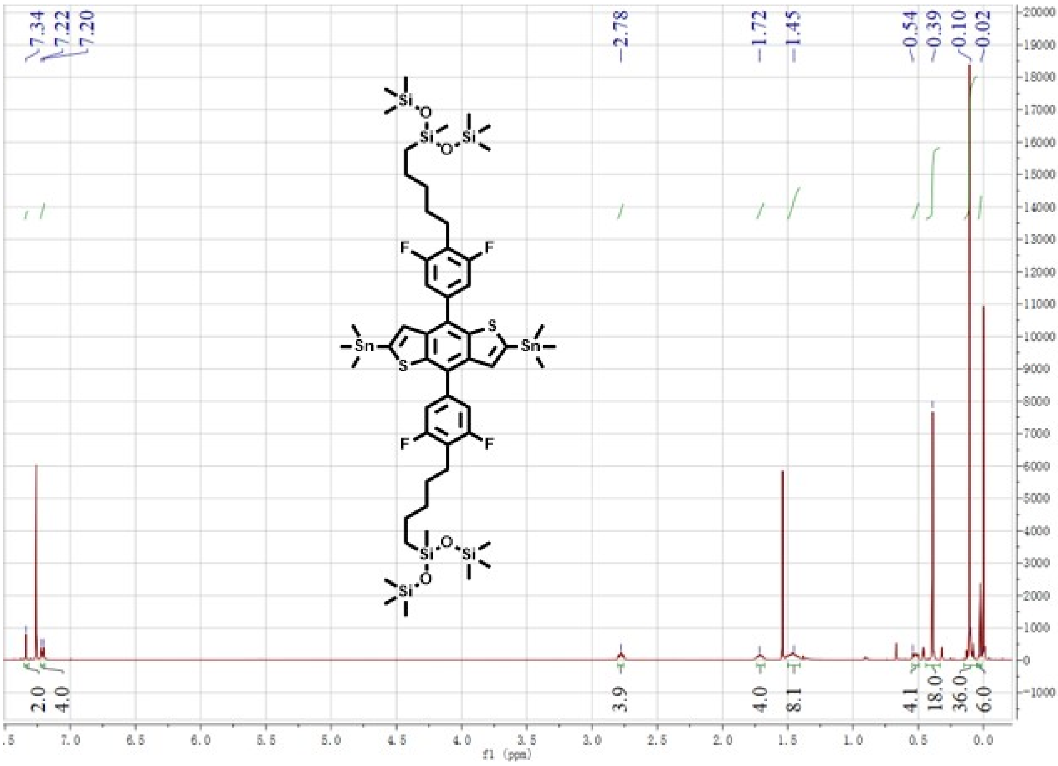

Figure S4. ^{1}H NMR spectrum of compound M1Si in $CDCl_3$.

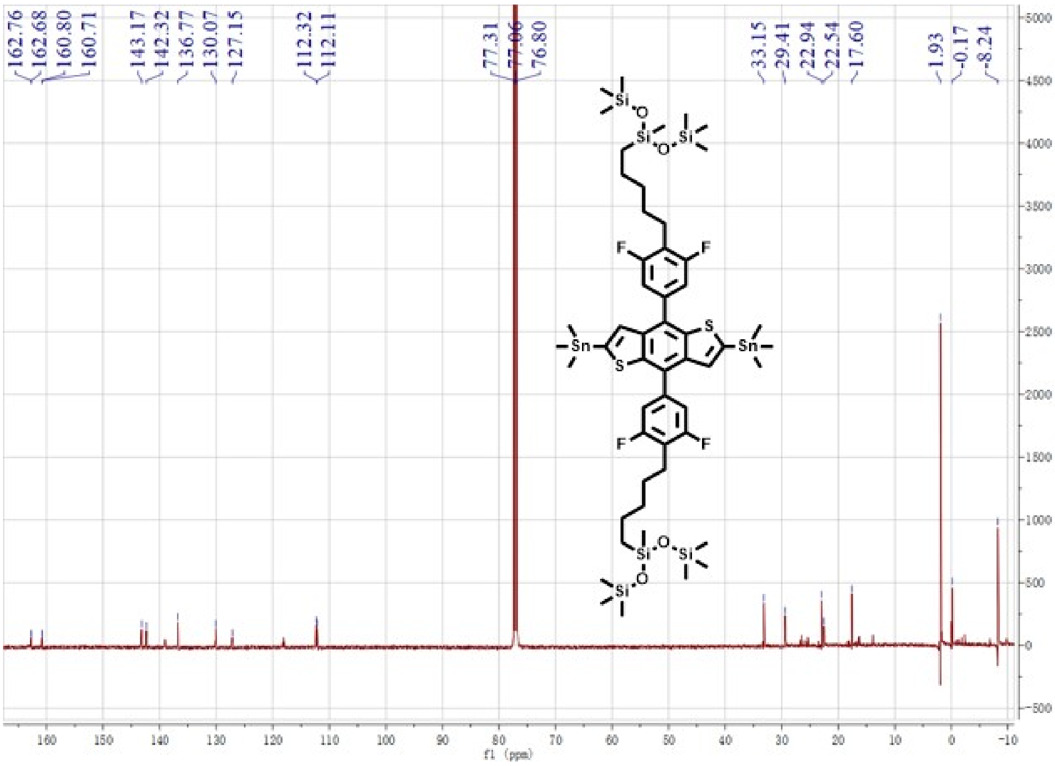

Figure S5. ^{13}C NMR spectrum of compound M1Si in $CDCl_3$.

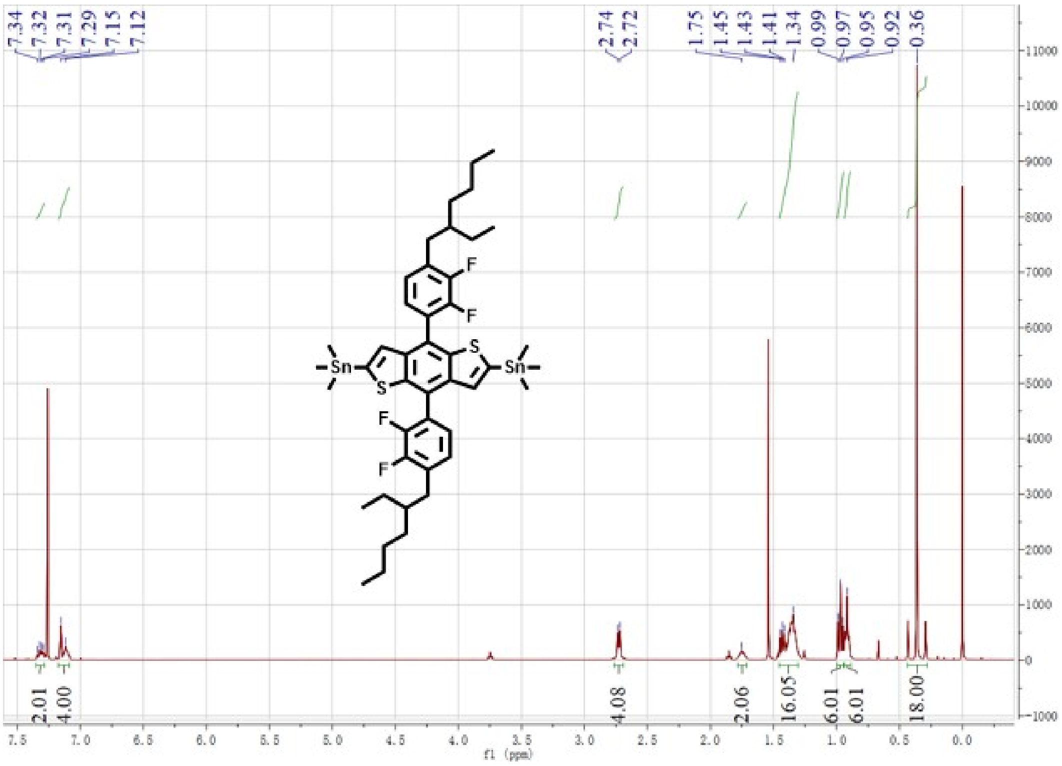

Figure S6. ^{1}H NMR spectrum of compound M2EH in $CDCl_3$.

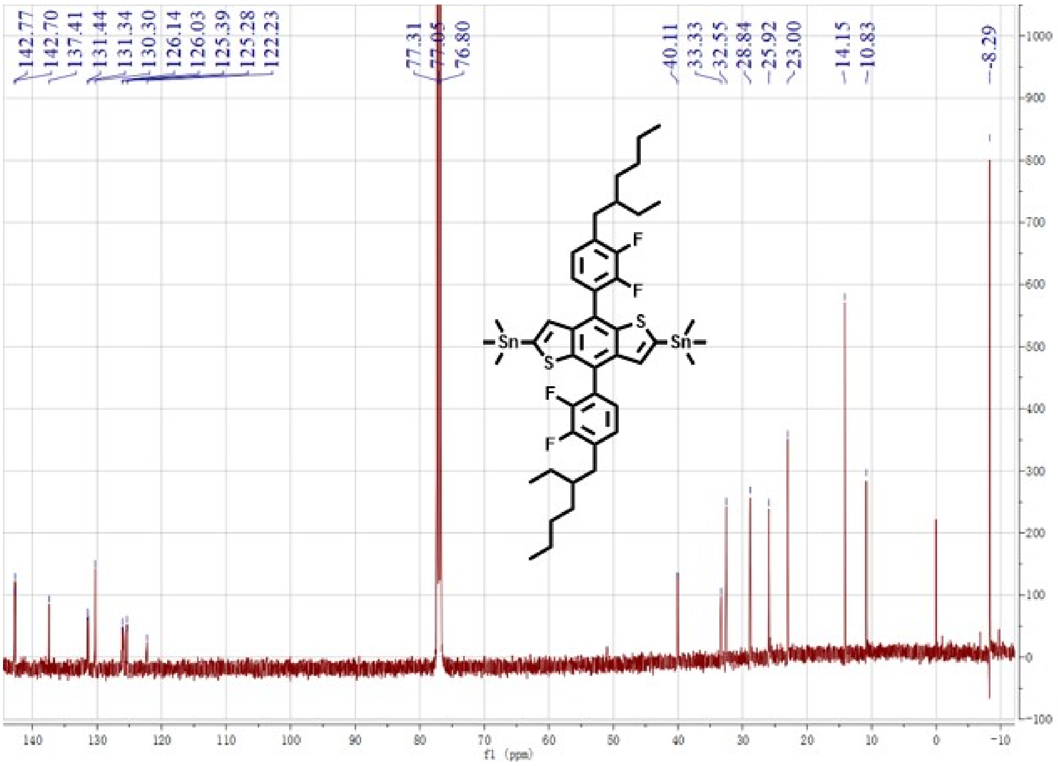

Figure S7. ^{13}C NMR spectrum of compound M2EH in $CDCl_3$.

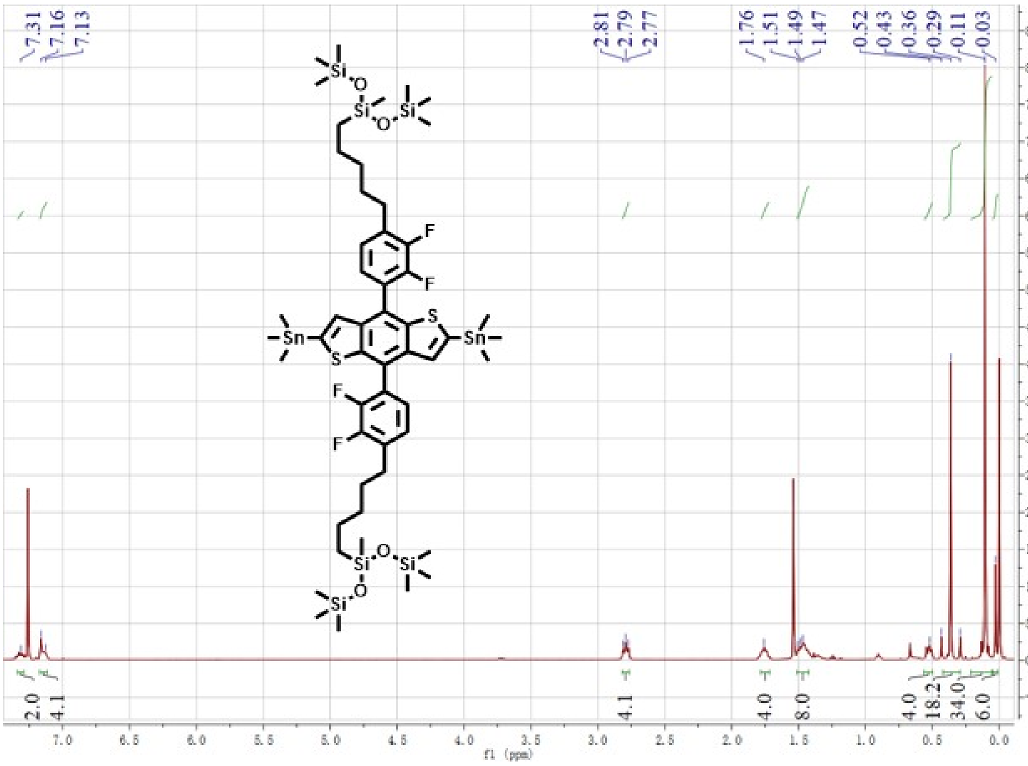

Figure S8. ^1H NMR spectrum of compound M2Si in $CDCl_3$.

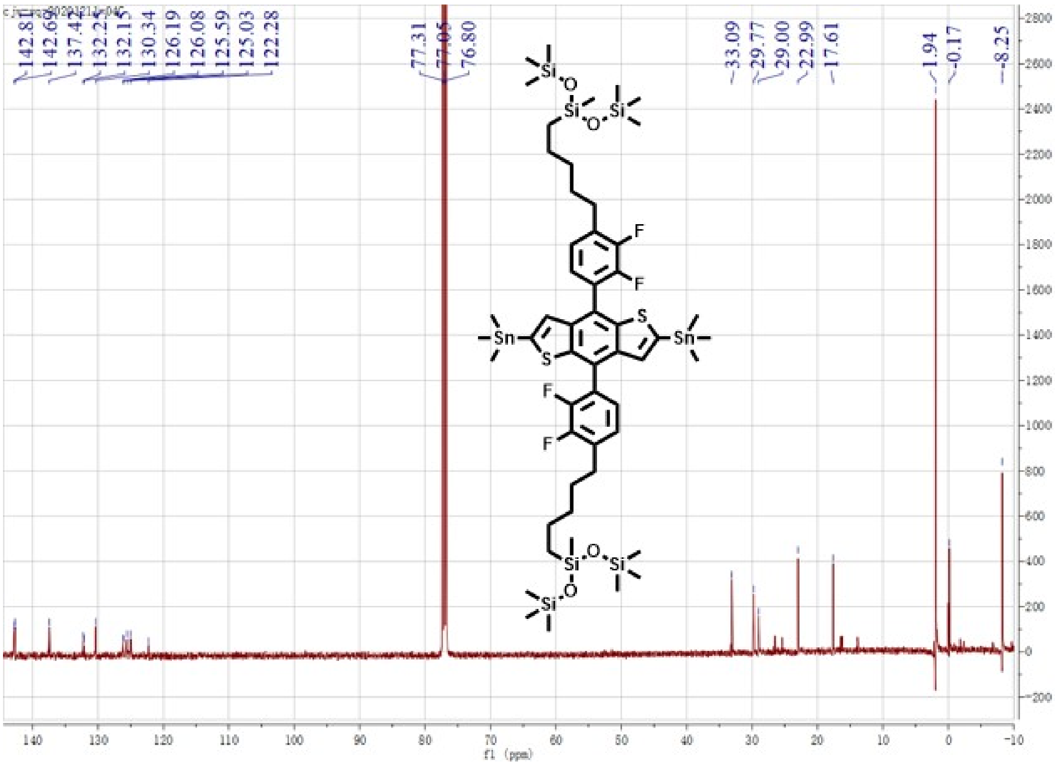

Figure S9. ^{13}C NMR spectrum of compound M2Si in $CDCl_3$.

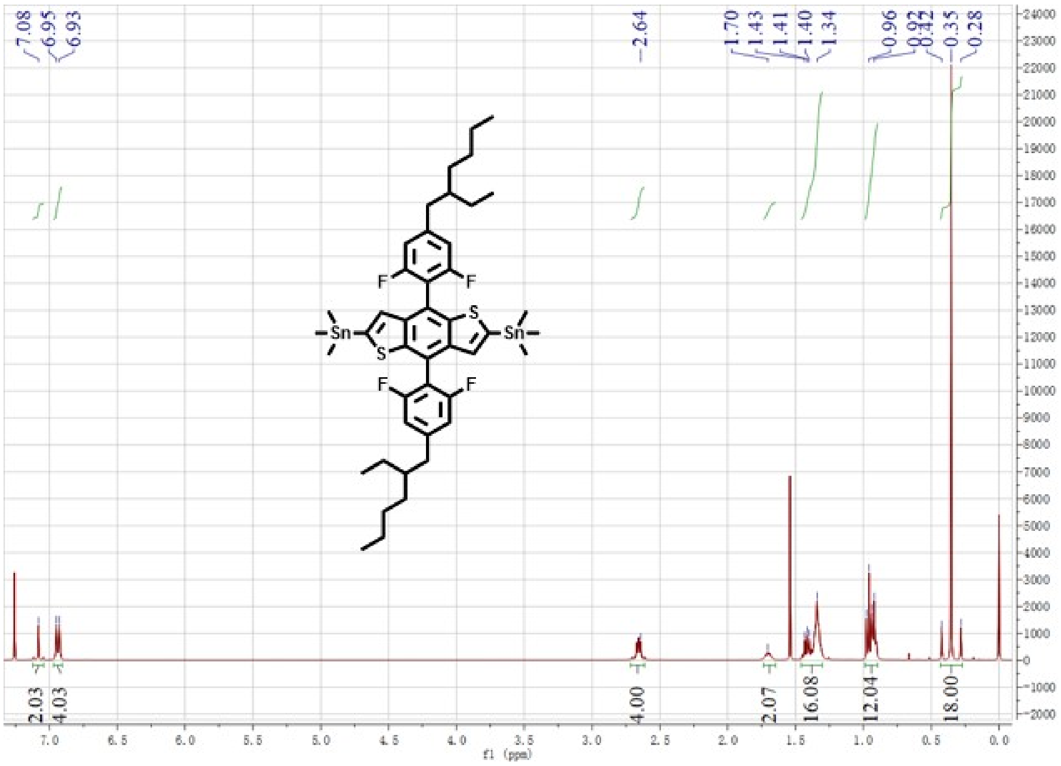

Figure S10. ^{1}H NMR spectrum of compound M3EH in $CDCl_3$.

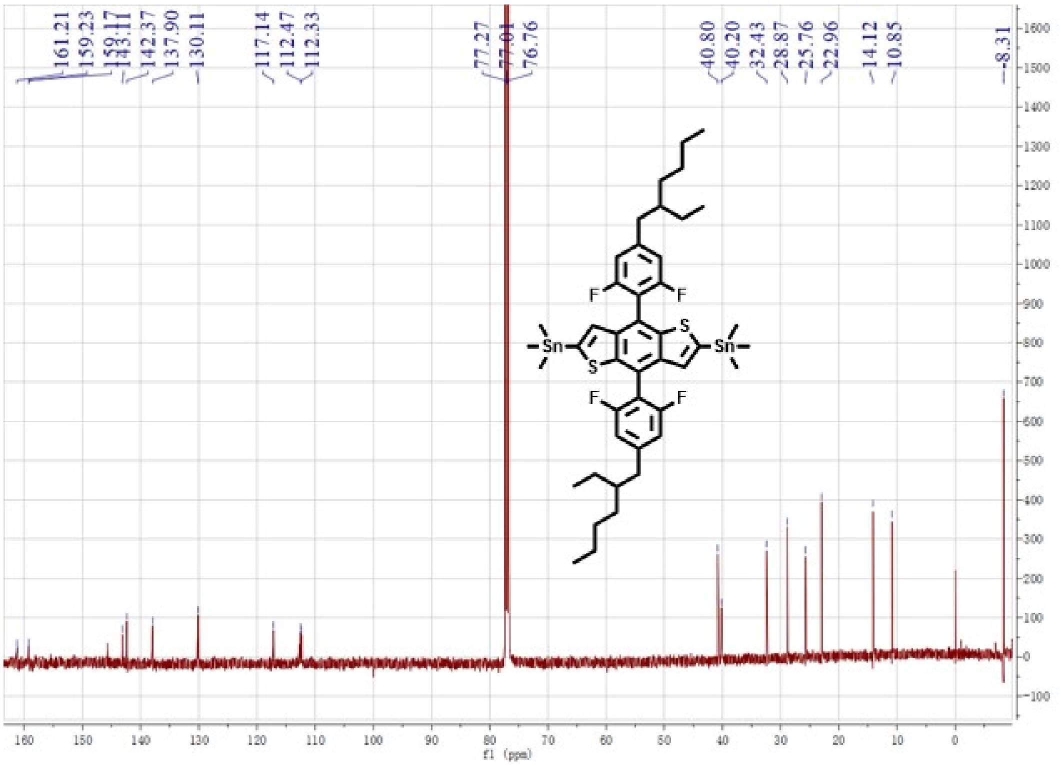

Figure S11. ^{13}C NMR spectrum of compound M3EH in $CDCl_3$.

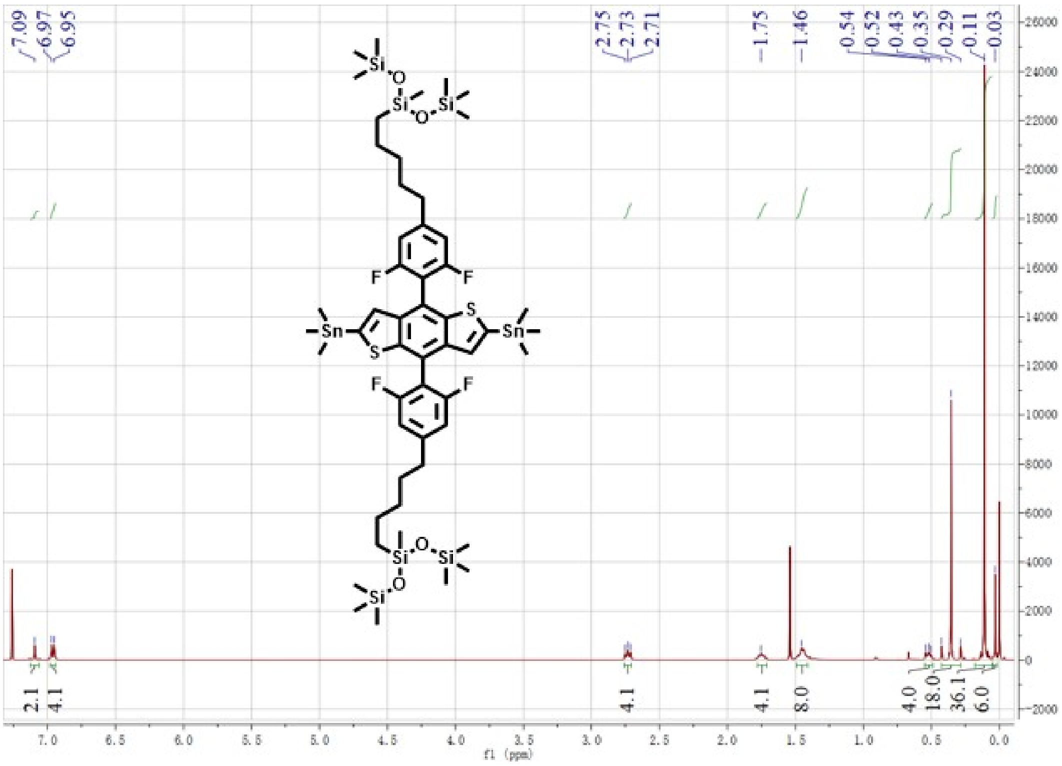

Figure S12. ^{1}H NMR spectrum of compound M3Si in $CDCl_3$.

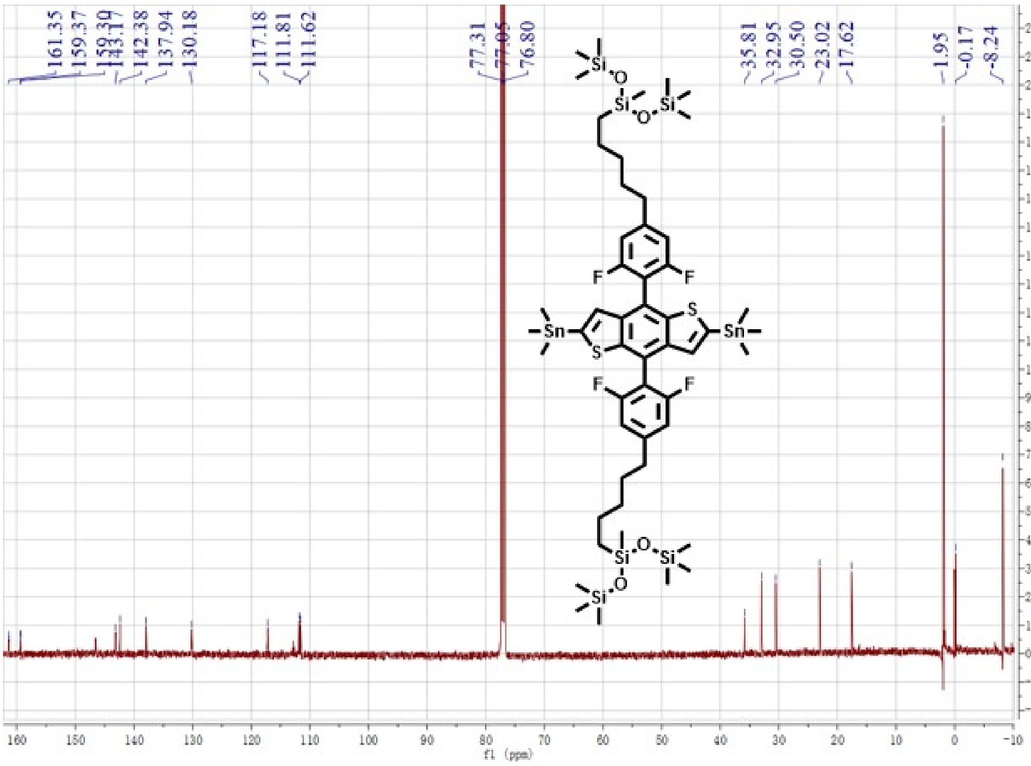

Figure S13. ^{13}C NMR spectrum of compound M3Si in $CDCl_3$.

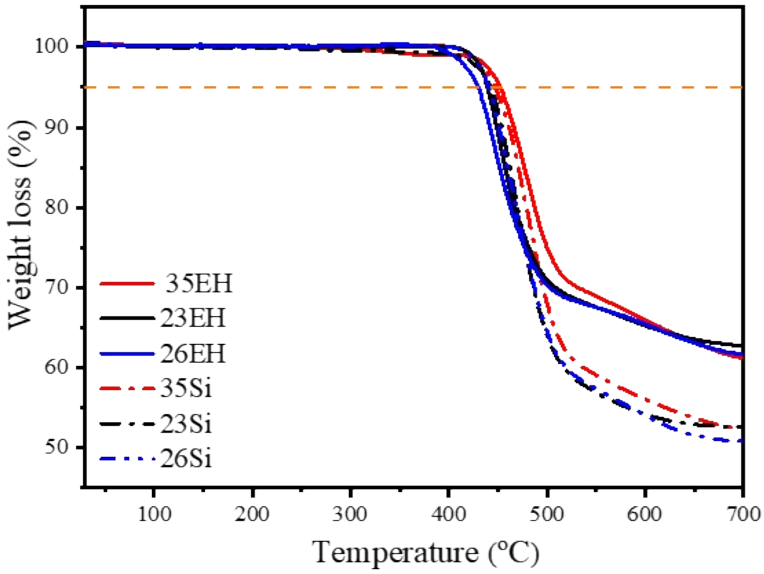

Figure S14. TGA plots of the polymers under N_2 atmosphere.

Table S1. Molecular weights and decomposition temperatures of the six polymers

Polymer	**M_n (kDa)**	**M_w (kDa)**	**PDI**	**T_d (°C)**
35EH	15.6	34.4	2.21	452
23EH	39.9	74.5	1.87	439
26EH	25.7	44.8	1.74	430
35Si	21.0	49.0	2.33	447
23Si	27.5	77.2	2.80	443
26Si	16.0	38.8	2.42	441

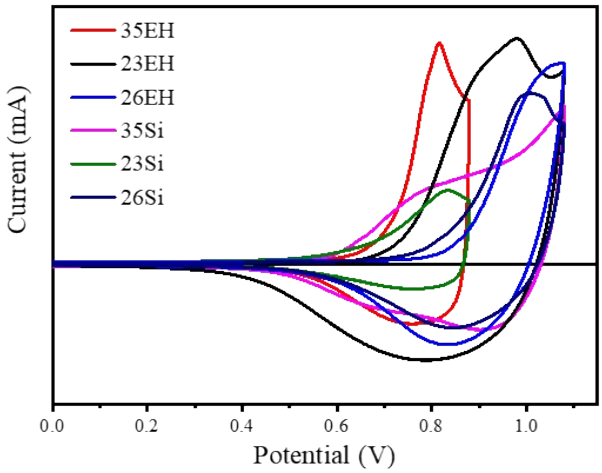

Figure S15. Electrochemical cyclic voltammetry (CV) curvers of polymer neat films.

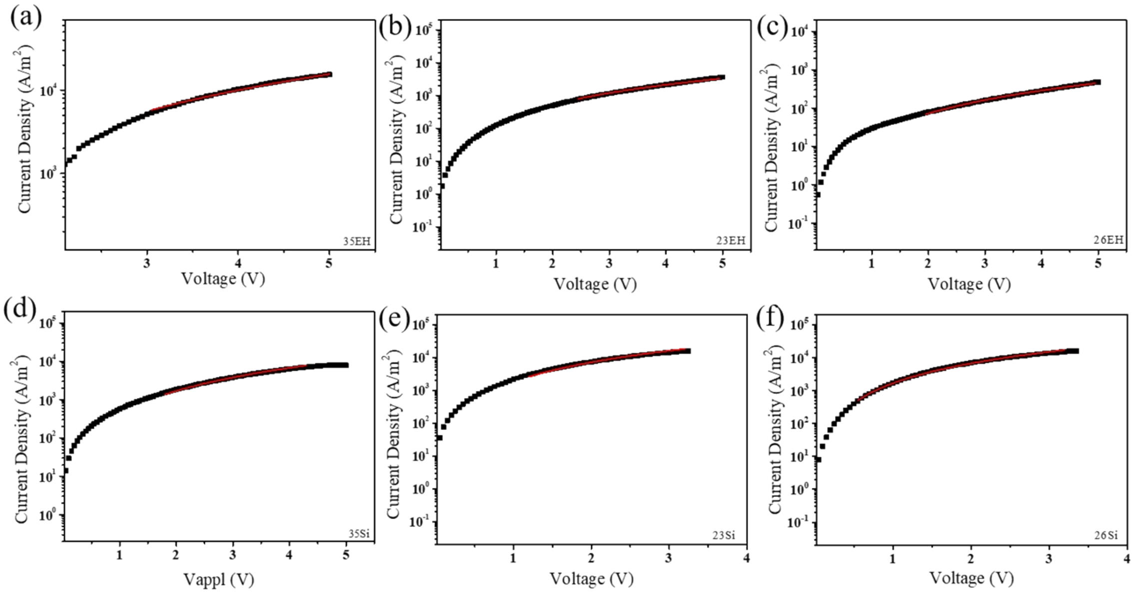

Figure S16. SCLC curves for hole-only devices based on: (a)35EH; (b) 23EH; (c) 26EH; (d) 35Si; (e) 23Si and (f) 26Si (the symbols are experimental data for transport of hole, and the red lines are fitted according to the space-charge-limited-current model).

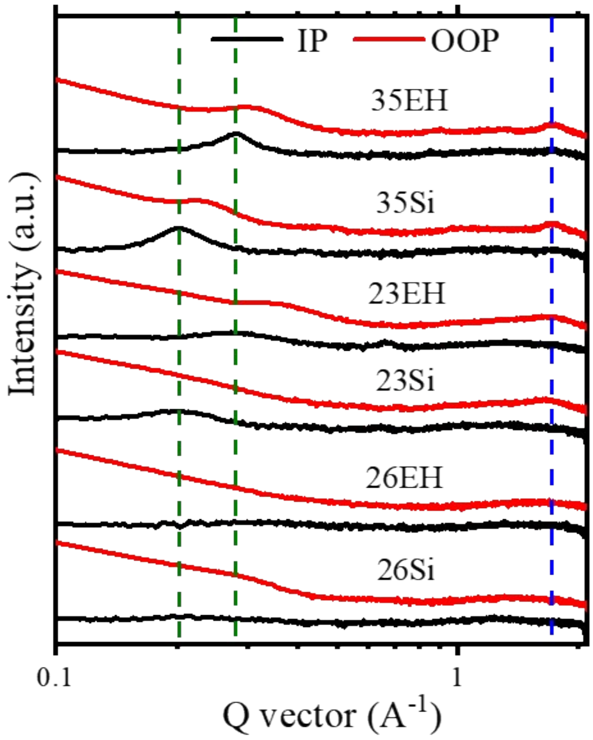

Figure S17. The GIWAXS line-cut profiles for the pristine polymer films.

Table S2. Summarized average parameters of the as cast neat film of polymers calculated from GIWAXS profiles

Polymer	**In plane (100) peak**		**Out of plane (100) peak**		**Out of plane (010) peak**	
	q_{xy} (Å^{-1})	***d*-spacing (Å)**	**q_z (Å^{-1})**	***d*-spacing (Å)**	**q_z (Å^{-1})**	**π-π distance (Å)**
35EH	0.280	22.43	0.305	20.59	1.723	3.64
35Si	0.202	31.10	0.238	26.40	1.729	3.63
23EH	0.279	22.51	0.358	17.54	1.717	3.67
23Si	0.200	31.42	——[a]	——[a]	1.717	3.67
26EH	——[a]	——[a]	——[a]	——[a]	——[a]	——[a]
26Si	——[a]	——[a]	——[a]	——[a]	——[a]	——[a]

[a] not detectable

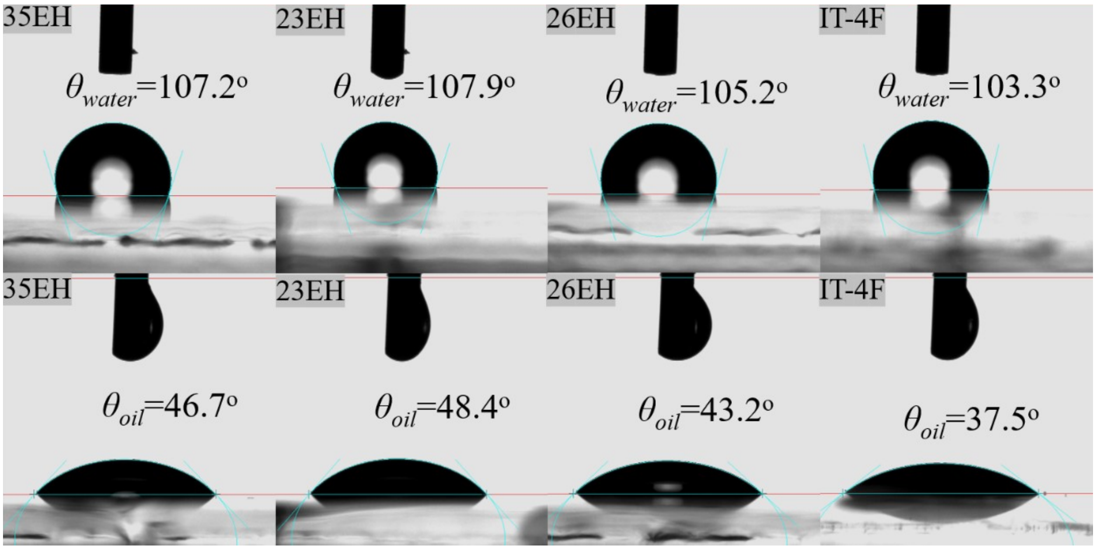

Figure S18. Views of surface contact measured by water and diiodomethane on the pristine films of polymer donors and IT-4F.

Table S3. The contact angles and surface energy parameters of the pristine polymer films measured by water and ethylene glycol

Surface	**Contact angle**		γ^p [b] **(mJ/m²)**	γ^d [b] **(mJ/m²)**	γ **(mJ/m²)**
	θ_{water} **(°)**	θ_{oil} **(°)** [a]			
35Si	106.7	48.3	36.00	0.085	36.08
23Si	107.2	49.2	35.57	0.098	35.67
26Si	105.9	48.4	35.47	0.038	35.51

[a] θ_{oil} represents the contact angle of ethylene glycol.

[b] γ^d and γ^p represent the surface free energies generated from the dispersion forces and the polar forces, respectively.

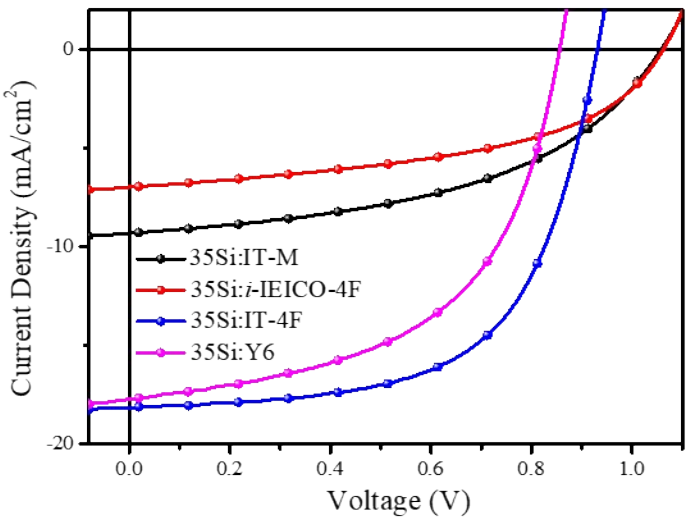

Figure S19. Current density-voltage (*J*-*V*) characteristics of the as-cast devices based on 35Si and different acceptors.

Table S4. Photovoltaic parameters of the as-cast devices based on 35Si and different acceptors

Active layer	V_{OC} (V)	J_{SC} (mA/cm^2)	FF (%)	PCE$_{max}$ (%)
35Si:IT-M	1.06	9.33	47.31	4.68
35Si:i-IEICO-4F	1.06	6.99	49.04	3.64
35Si:IT-4F	0.93	18.17	61.05	10.32
35Si:Y6	0.86	17.74	53.60	8.19

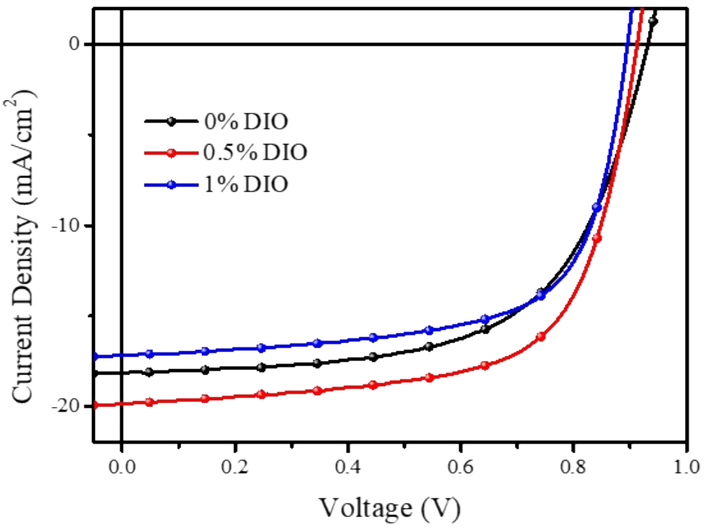

Figure S20. Current density-voltage (*J*-*V*) characteristics of the 35Si:IT-4F (1:1) based devices with different addition of DIO.

Table S5. Photovoltaic parameters of the 35Si:IT-4F (1:1) based devices with different addition of DIO

DIO	V_{OC} **(V)**	J_{SC} **(mA/cm^2)**	**FF (%)**	**PCE$_{max}$ (%)**
0	0.93	18.17	61.05	10.32
0.5%	0.91	19.85	66.42	12.01
1%	0.89	17.15	67.61	10.33

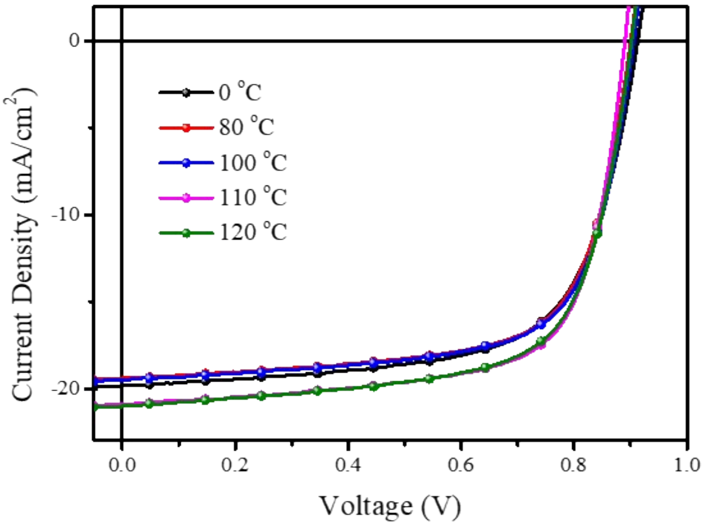

Figure S21. Current density-voltage (*J-V*) characteristics of the 35Si:IT-4F (1:1) based devices under different post-annealing temperature.

Table S6. Photovoltaic parameters of the 35Si:IT-4F (1:1) based devices under different post-annealing temperature

Temperature (°C)	V_{OC} **(V)**	J_{SC} **(mA/cm^2)**	**FF (%)**	**PCE$_{max}$ (%)**
0	0.91	19.85	66.42	12.01
80	0.90	19.41	68.85	12.04
100	0.90	19.53	68.85	12.11
110	0.89	20.93	69.58	12.97
120	0.90	21.02	67.76	12.83

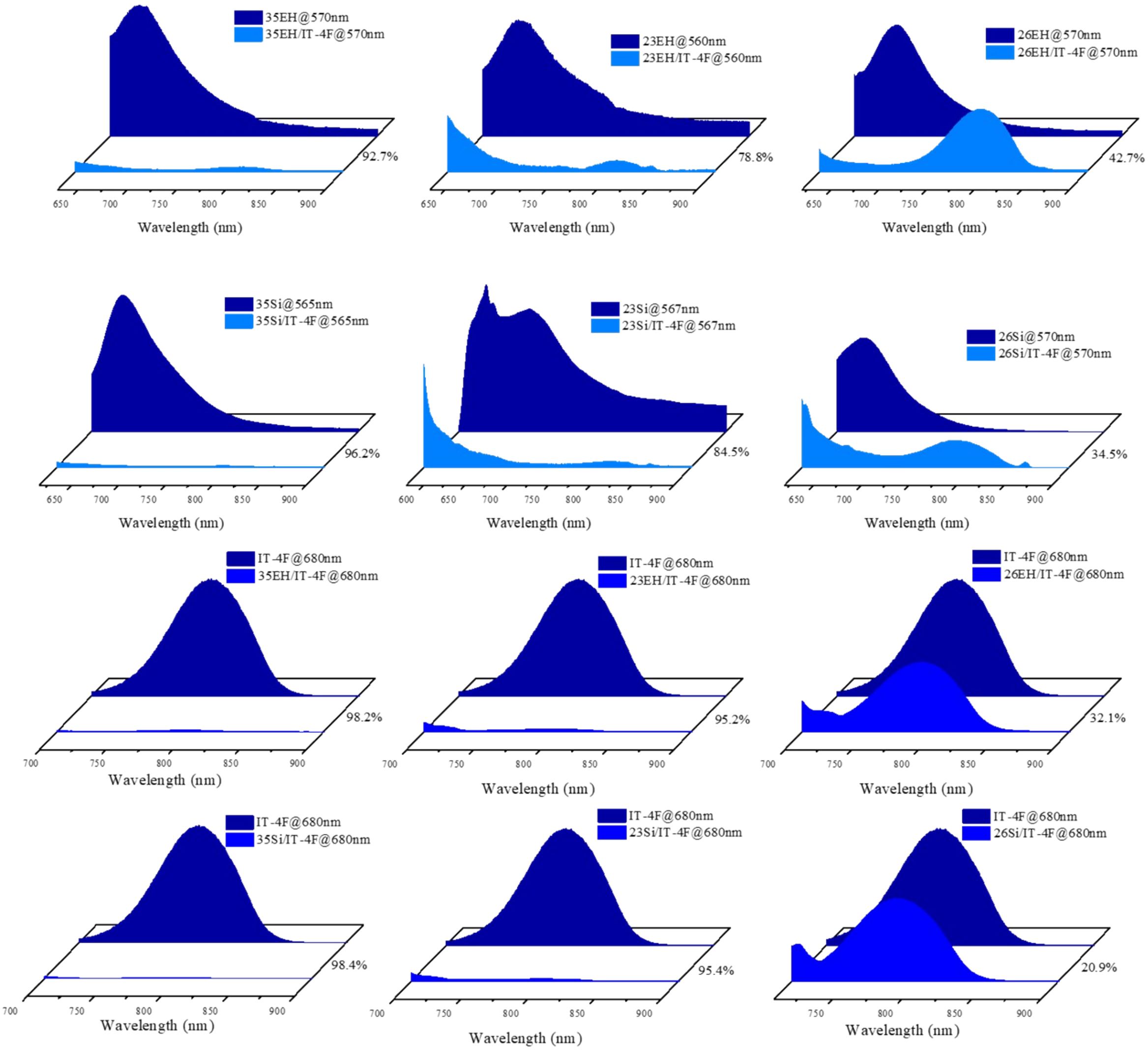

Figure S22. PL spectra of the pristine and blend films.

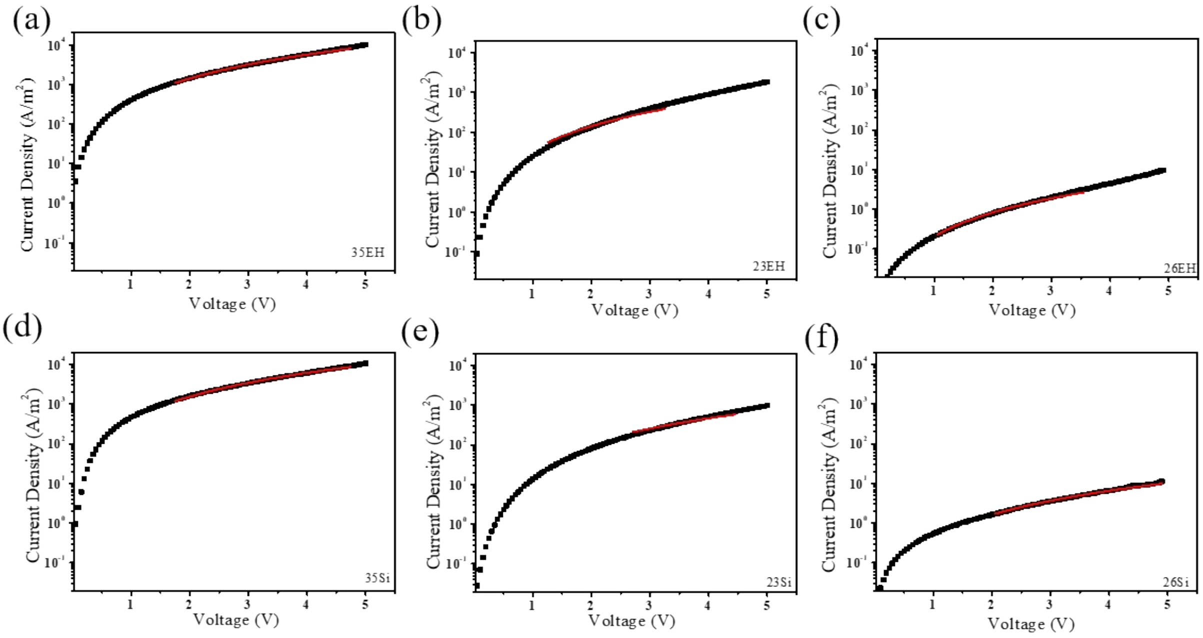

Figure S23. SCLC curves for hole-only optimized devices based on: (a)35EH:IT-4F, (b)23EH:IT-4F, (c)26EH:IT-4F, (d)35Si:IT-4F, (e)23Si:IT-4F and (f)26Si:IT-4F. (The symbols are experimental data for transport of hole/electron, and the red lines are fitted according to the space-charge-limited-current model).

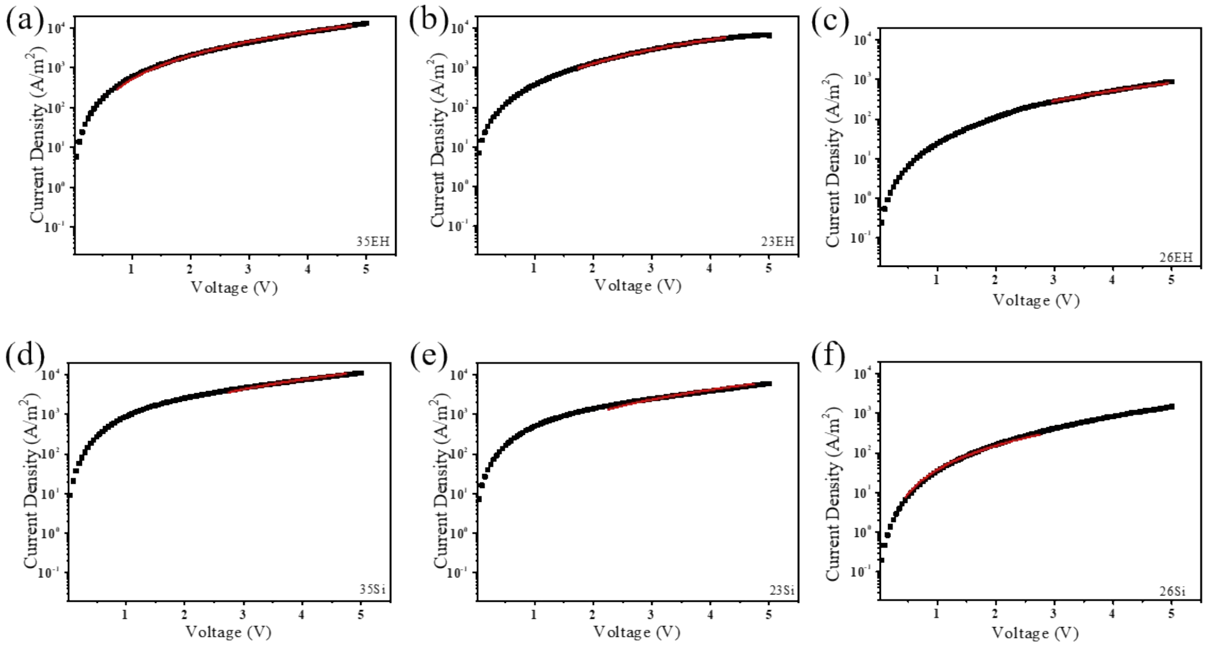

Figure S24. SCLC curves for electron-only optimized devices based on: (a)35EH:IT-4F, (b)23EH:IT-4F, (c)26EH:IT-4F, (d)35Si:IT-4F, (e)23Si:IT-4F and (f)26Si:IT-4F. (The symbols are experimental data for transport of hole/electron, and the red lines are fitted according to the space-charge-limited-current model).

Table S7. Summarized average parameters of the blend films calculated from GIWAXS profiles

Polymer:IT-4F	**In-plane (100) peak**		**Out-of-plane (100) peak**		**Out-of-plane (010) peak**	
	q_D/q_A (Å^{-1})	***d*-spacing (Å)**	**q_z (Å^{-1})**	***d*-spacing (Å)**	**q_z (Å^{-1})**	**π-π distance (Å)**
35EH:IT-4F	0.280/0.322	22.43/19.50	0.305	20.59	1.790	3.50
23EH:IT-4F	—/0.322	—/19.50	0.324	19.38	1.808	3.47
35Si:IT-4F	0.202/0.324	31.09/19.38	0.225	27.91	1.821	3.45
23Si:IT-4F	0.212/0.321	29.62/19.56	0.245	25.63	——[a]	——[a]
26EH:IT-4F	—/—[a]	—/—[a]	——[a]	——[a]	——[a]	——[a]

[a] not detectable